Polymer Testing 111 (2022) 107619

Contents lists available at ScienceDirect

Polymer Testing

journal homepage: www.elsevier.com/locate/polytest

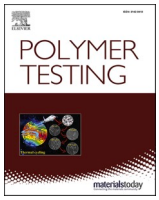

Behaviour of a self-reinforced polylactic acid (SRPLA) in seawater

M. Le Gall [a], Z. Niu [b], M. Curto [c], A.I. Catarino [b], E. Demeyer [d], C. Jiang [c], H. Dhakal [c], G. Everaert [b], P. Davies [a,*]

[a] IFREMER Centre Bretagne, Marine Structures Laboratory, Technopole Iroise, 29280, Plouzané, France
[b] Flanders Marine Institute (VLIZ), Wandelaarkaai 7, 8400, Oostende, Belgium
[c] School of Mechanical and Design Engineering, University of Portsmouth, PO1, 3DJ, UK
[d] CENTEXBEL – VKC, Etienne Sabbelaan 49, BE 8500, Kortrijk, Belgium

ARTICLE INFO

Keywords:
Polylactic acid
Marine environment
Mechanical properties
Durability
Microplastics
Moisture absorption

ABSTRACT

The goal of this study was to determine whether a bio-based self-reinforced polylactic acid (SRPLA) is suitable for use in structures deployed in the marine environment. The material was produced from co-mingled fibres with different melting points. Two key criteria, durability during service and microplastic formation, were examined. To assess durability, mechanical properties, tension and transverse impact, were used to quantify the influence of seawater ageing for up to 24 months. After seawater ageing at 40 °C for 12 months, composite strength was completely degraded. To assess microplastic formation, specimens of SRPLA were exposed in seawater to accelerated ultraviolet (UV) radiation simulating natural exposure for up to 18 months. Fluorescence microscopy and infrared technology were used to quantify and characterise the microplastics formed. Their number was independent of UV exposure, suggesting short-term UV radiation does not accelerate SRPLA microplastic formation. We discuss the potential for SRPLA to be considered a promising material for sustainable marine applications.

1. Introduction

The replacement of petrochemical based polymers by bio-based polymers offers the potential to reduce environmental impact through reduced energy requirements and carbon footprint. When bio-based polymers are bio-degradable, through composting or other processes, this can also significantly improve end of life conditions and further reduce negative environmental impacts. As a result, fully recyclable poly (lactic) acid, PLA, has received considerable attention. This polymer was first synthesised in 1845 but it was not until the 1990's when Cargill and Dow Chemicals industrialised the process [1], and set up the Nature-Works™ company, that it became widely available. It is a biobased, compostable, semi-crystalline polymer which has found many applications from packaging to medical components [2].

Polymers exhibit remarkable properties such as low weight and ease of manufacturing, but their stiffness and strength remain low compared to traditional structural materials. Fibrous reinforcement with glass or carbon fibres can improve properties significantly but may complicate end of life recovery due to the different natures of the components. If polymers can be reinforced by fibres with the same molecular chemistry then these drawbacks may be overcome, and this has led to the development of a class of materials known as self-reinforced (SR) polymers. The most common approach is to use a polymer with two melting points, fibres with a high melting temperature (Tm) and matrix with a lower Tm. The SR polymer is manufactured by forming at an intermediate temperature. After early work by Capiati and Porter on model polyethylene composites with two melting temperatures [3] various SR polymers were developed [4,5]. In addition to polyethylene [3,6,7], polypropylene (PP) reinforced by PP fibres has been examined in detail [8–11], while polyethylene terephthalate (PET) [12,13], polymethyl methacrylate (PMMA) [14] and cellulose [15–17] have also been studied. Published results for these SR polymers have shown good fibre/-matrix adhesion with significant strength and stiffness improvements compared to the parent materials [e.g. 4].

Another member of this family is SRPLA, composed of PLA matrix reinforced by PLA fibres. It is receiving current attention due to environmental impact concerns, but it was studied previously for medical applications. For example, Majola et al. described a study of SR PLLA and SR PDLLA/PLLA rods as fixation structures for bone surgery [18], while Wright-Charlesworth et al. examined processing effects using

* Corresponding author.
E-mail address: peter.davies@ifremer.fr (P. Davies).

https://doi.org/10.1016/j.polymertesting.2022.107619
Received 7 January 2022; Received in revised form 21 April 2022; Accepted 2 May 2022
Available online 5 May 2022

nano-indentation [19]. More recently, Mai et al. developed a manufacturing process for this material in order to overcome the brittleness and low thermal stability of PLA [20]. They produced PLA films by extrusion, and then oriented them by drawing them at temperatures below their melt temperature. The resulting properties depend on the drawing temperature but in their work maximum tape stiffness and strength of 6.7 GPa and 278 MPa respectively were obtained. These values are similar to other published values for drawn PLA. They are lower than those obtained for PE and PP but the theoretical crystal modulus for PLA is also much lower, around 12 GPa, [21]. Laminates were produced by stacking oriented and matrix layers in a hot press. Other recent work has been presented on PLA nano-fibre reinforced PLA [22].

The self-reinforced PLA composites studied in the present work were developed within the European BIO4SELF project [23–25] and were then studied further within the EU SeaBioComp project [26]. The manufacturing approach uses co-mingled fibres of two melting temperatures, 177 °C and 125–135 °C. Unidirectional SRPLA panels were produced by heating just below the melt temperature of the higher melting fibres and consolidating in a press. Measured strength values in the oriented direction of 107 MPa were around twice those of the unreinforced PLA, but lower than theoretical predictions. Very large strains to failure were obtained, over 30%, indicating that the SRPLA approach was able to overcome intrinsic PLA brittleness.

Plastics are extensively used in marine applications and there is strong concern over their degradation with time, both with respect to in-service performance and to possible marine pollution. For this reason, it is important to understand the mechanisms of degradation and their kinetics before using a new material at sea. The present paper investigates the potential of SRPLA for marine applications such as port infrastructure, buoys and pleasure boat structures. These marine structures are subjected to various mechanical constraints, with impact resistance being particularly important. The relevant background to this work therefore covers previous seawater ageing studies, impact behaviour and microplastic formation of SRPLA materials in a marine environment.

The behaviour of PLA alone in humid environments has been examined in some detail, as it is one of the elements of the composting environment. For example, parametric studies on PLA grades and environmental conditions are available [27,28]. However, degradation studies of PLA in seawater are less common. Le Duigou et al. [29] examined unreinforced and flax fibre reinforced composites in seawater. For their unreinforced polymer (injection moulded L9000 grade from Biomer™) saturation weight gain at 40 °C was low, around 0.65%. After 3 months in water at 40 °C (at saturation) a loss in strength of around 30% was observed. Deroiné et al. [30] compared distilled water and seawater degradation of another PLA (7001D from NatureWorks™) after six-month immersions at different temperatures. They showed strong drops in strength and failure strain at 40 °C but little change for this duration at 25 °C.

Previous work on the influence of moisture on SRPP materials showed significant water uptake due to the presence of voids but little influence on mechanical properties [31]. For SRPLA however, although some mechanical properties are given in Refs. [20,23], few long term properties are available. An exception is the recent work on biodegradation of polymers from renewable resources [32] and particularly SRPLA [33]. This described results for three test conditions, composting, immersion in ultra-pure water and thermal ageing, all at 58 °C. For the materials studied significant degradation occurred fastest under composting conditions, more slowly in water and not at all under thermal ageing alone.

Very few studies have examined the impact behaviour of self-reinforced polymers. Alcock et al. [34] provided results for ballistic impact of SRPP and showed that they retained good impact resistance even at low temperatures. Aurrekoetxea et al. [35] presented a study of falling weight impact on 2.2 mm thick woven SRPP composites, and indicated damage and perforation thresholds of 5 and 31 J. Santos et al. also used a falling weight tower to compare the penetration impact behavior of five commercially available self-reinforced composites with thicknesses from 0.5 to 2.1 mm, based on PP and PET [36]. They found significant differences in penetration impact resistance, from 15 to 40 J/mm. Mai et al. examined energies absorbed during impact on SRPLA and revealed an increase of 14 times compared to unreinforced PLA [20].

Microplastics, i.e. plastic particles smaller than 5 mm in diameter, are ubiquitous in the global ocean [37]. An important source of microplastics in the marine environment is particles fragmented and released from larger-sized plastics under a combination of physical, chemical and biological forces [37]. Therefore, when assessing the characteristics of SRPLA applications deployed in seawater, attention should be given to their potential of releasing microplastics, due to concerns on toxicological and environmental impacts [38,39]. Ultraviolet (UV) radiation, the trigger to initialise the abiotic degradation of plastics, is considered as the leading force for microplastic formation [42,43]. A number of studies have provided evidence of microplastics released from conventional plastics under UV radiation in laboratory conditions, observed via weight loss, changes in average particle size and SEM observations [43–46]. However, quantitative evidence of microplastic formation after UV radiation is limited, especially for bio-based composites [47,48]. To date only a few studies have assessed the disintegration of PLA and its capacity to form microplastics; for example [47] where the author found 425 and 20,000 PLA microplastics (2–60 μm)/L released from samples in the dark and subject to 56-day UV radiation, respectively. The quantification and characterisation of microplastics formed from SRPLA is a key element to assess the sustainability of future SRPLA applications and to support a transition process to improved plastic materials.

Although the behaviour of SRPLA materials in a marine environment has received little attention to date, it is important to examine as it is anticipated that their future use in the marine environment will significantly increase after the implementation of new EU legislation on single use plastics [49]. Therefore, in the present research we aim to: 1) Evaluate the seawater diffusion kinetics; 2) Quantify the influence of seawater on mechanical behaviour, and 3) Examine the formation of microplastics under solar radiation. We believe that this information is essential for both designers and end-users and will lead to improved marine applications.

2. Materials and methods

The material tested in this work was manufactured from two co-mingled grades of PLA fibres, with a 50:50 mixing ratio woven in a 0/90° configuration with a fine weave (twill 2/2, 680 g/m^2 and a repeat element around 2 mm × 2 mm) and press formed at 160 °C. The 4000 dtex fibres show diameters around 21 μm (Fig. 1a). The composite was supplied as sheets of three woven layers with a 1.3 mm thickness (Fig. 1b).

2.1. Tensile tests

In an initial material characterisation tensile tests were performed on the unaged high Tm fibres (Fig. 1a), using pneumatic yarn grips. The distance between grips was 500 mm, loading rate was 50 mm/min, and strain was measured by following markers on the fibres with two digital cameras and image analysis. To determine a modulus value, the applied stress σ is needed; this was obtained from the applied load F, the density ρ (measured by gas pycnometer) and the measured linear weight in tex (g/km) using the expression:

$$\sigma = \rho F(N)/\text{linear weight(tex)}$$

Fig. 2 shows the fibre behaviour. Based on these results from 5 tensile

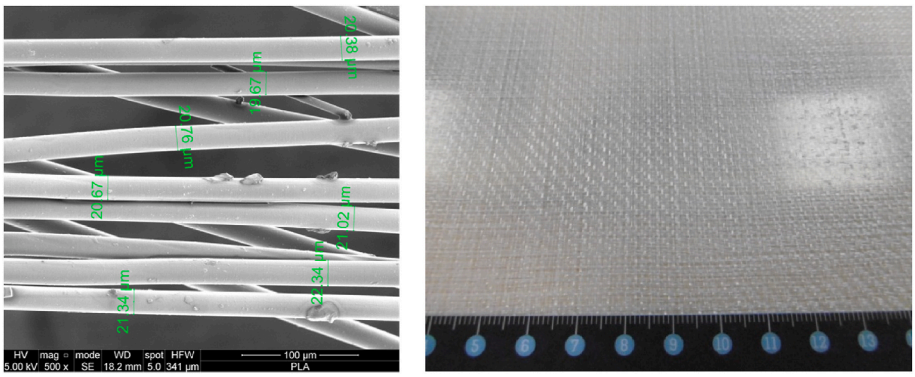

Fig. 1. Material studied, a) High Tm PLA fibres, b) SRPLA sheet.

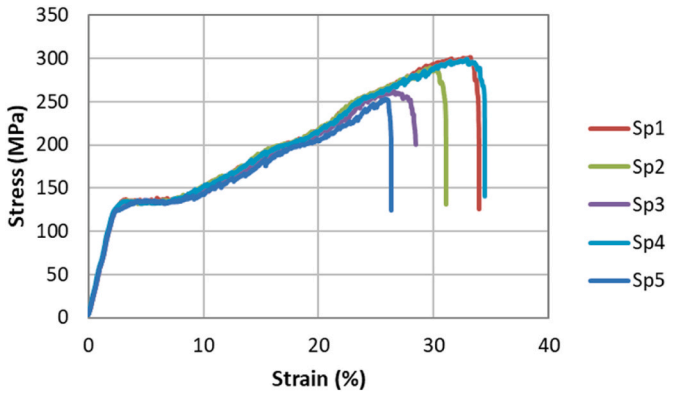

Fig. 2. Tensile properties of high melting temperature PLA yarns.

tests on the unaged fibres, we determined an initial axial modulus around 5.6 GPa (Table 1).

The mechanical properties of the low Tm fibres were lower than the detection limit of the equipment used. Hence, no results are shown for these samples.

SRPLA tensile tests were performed on ISO 527 type 5A dogbone specimens cut from the sheets with a die punch. For each test condition eight specimens were prepared, four were tested with a clip-on Instron™ extensometer and four without. This allowed modulus to be determined from the initial stress-strain slope together with strain to failure on four specimens and break stress to be measured without the influence of the extensometer on four others. Crosshead displacement rate was 2 mm/min. Tests after ageing were performed on wet specimens unless specified; specimens were removed from ageing tanks then kept in water until mounting on the test frame. Additional analyses of mechanical test specimens were performed by calorimetry (TAI Q200™ DSC equipment under nitrogen), at a heating rate of 10 °C/min. Scanning Electron Microscopy (SEM) observations were made on Au–Pd coated samples in a FEI Quanta™ 200 microscope.

Table 1
Initial properties of reinforcement fibres and SRPLA in 3 directions, mean (standard deviation).

	Modulus, (GPa)	Break stress, (MPa)	Break strain, (%)
Fibre high Tm	5.60 (0.70)	281 (22)	31 (4)
Typical bulk amorphous PLA [53]	3.5	59	7
SRPLA 0°	2.75 (0,02)	37.6 (0.7)	25 (2)
SRPLA 90°	2.42 (0.21)	35.0 (1.3)	27 (2)
SRPLA 45°	1.89 (0.04)	31.4 (0.5)	31 (2)

2.2. Seawater ageing

Seawater ageing was performed in temperature-controlled tanks at the Ifremer Centre, supplied with natural seawater pumped from the Brest Estuary (France). The water was continuously renewed and the tanks used in this work were maintained at 4, 15, 25, 40, 60 and 80 °C ± 2 °C. The immersed coupon dimensions were 50 x 50 mm^2. It is important that these be sufficiently large to limit edge effects [50,51]. They were removed periodically for weighing on a Sartorius™ balance. For each test condition 5 coupons were weighed.

2.3. Additional ageing conditions

In addition to these seawater ageing tests two extra series were performed. First, a set of specimens was held at 40 °C in an oven for 9 months before testing, to examine whether the temperature alone affected the tensile behaviour. Second, another unaged reference series was tested at the end of the ageing period, one year after the initial tests, to check that the material had not changed with time during room temperature storage.

2.4. Falling weight impact tests

The impact damage behaviour of the SRPLA has been characterised by drop weight impact tests. An Instron CEAST™ 9350 low-velocity falling weight impact tower was employed with a hemispherical nose impact tup with a diameter of 20 mm. The machine was equipped with an anti-rebound system. Three different incident impact energies were employed from barely visible damage up to penetration. Impact tests were performed on square specimens of dimensions 100 mm by 100 mm with thickness of 1.3 mm. The test specimens were clamped on a rigid metallic support ring of 20 mm, and incident energies ranged from 5 to 15 J. The different energy values were obtained by adjusting the drop height of the impact mass (3.15 kg). For each incident energy level five samples were tested dry and five after ageing under each of two conditions; immersion in sea water at 25 and 40 °C for 40 days. Samples were removed from the 15 J impact samples, coated under vacuum with a 1 µm thick gold-palladium coating using a Quorum™ Q150 R–S rotary pumped coater. Sample images were recorded at a magnification of 40 and 200 X with a ZEISS™ EVO MA10 scanning electron microscope.

2.5. Assessment of microplastics formation

The UV exposure experiment was performed in an Atlas Suntest CPS + instrument fitted with a Xenon lamp (1500 W) and daylight filter, with the emission range at 300–400 nm. Irradiation intensity was conducted at 60 W/m^2 and the temperature in the chamber was maintained at 35–38 °C. Prior to exposure, SRPLA sheets were cut into 0.15 x 2 × 4 cm flakes using a stainless-steel scissor, and thoroughly rinsed with

Milli-Q water (Millipore Corporation). To avoid releasing particles due to the mechanical stress induced by cutting manipulation, the edges of the flakes were smoothed using a hot knife. Each flake was placed in a pre-cleaned 25 mL quartz cuvette and immersed with 20 mL artificial seawater that was prepared according to ISO 10253:2016 [58] and filtered through a 0.2 μm PTFE filter. Triplicated samples (i.e. in total 12 cuvettes) were subjected to UV exposure for 77, 458, 917, and 1368 h, which corresponded to 1, 6, 12, and 18 months of central European solar irradiance exposure, respectively [44]. Dark control samples (n = 3) were wrapped with aluminium foil and incubated in the same conditions for 1368 h. Loss of water by evaporation was compensated by regularly supplying vials with Milli-Q water. After sampling, water samples were filtered through 0.2 μm Whatman® PTFE filter, stained with 1 mL Nile Red (10 μg/mL in acetone) and stored at room temperature in the dark until further analysis. The formed microplastic from SRPLA flakes were identified using a combination of fluorescent microscopy and image analysis (details given in SI). Several Quality Criteria and Quality Control measures, recommended in de Ruijter et al. [52] were implemented during the experimental procedures to avoid contamination of the samples by airborne fibres and other particles (details provided in SI). A blank procedure (i.e., 20 mL Milli-Q water) was carried out prior to each sample test to account for background PLA contamination.

The microplastic formation dataset (i.e. the number of microplastics formed at each UV radiation time) was analysed using a non-parametric test as the ANOVA assumption of normality was not met. To do so, a Kruskal-Wallis Rank Sum Test was performed to if there were significant differences in the number of microplastics formed in each time treatment ($\alpha = 0.05$). A Dunnett test was applied to compare the variance in number of microplastic particles between the treatment and control. Statistical analysis was performed in R, v3.6.1 [59].

3. Results

- *Initial mechanical properties*

First, tensile tests were performed on the unaged SRPLA, and properties in the 0°, 90° and 45° directions were determined, Fig. 3 and Table 1.

The main benefit in adding fibres to PLA matrix is an increase in stiffness in the fibre directions. Strains to failure in all three directions are also significantly higher than values usually cited for unreinforced PLA (<10% elongation). More significant stiffness improvements were found previously for unidirectional composites based on the same comingling process [23]. There is a small (around 10%) difference in properties between the 0° and 90° directions (Fig. 3); for the subsequent ageing studies all specimens were cut in the 0° direction.

- *Seawater ageing*

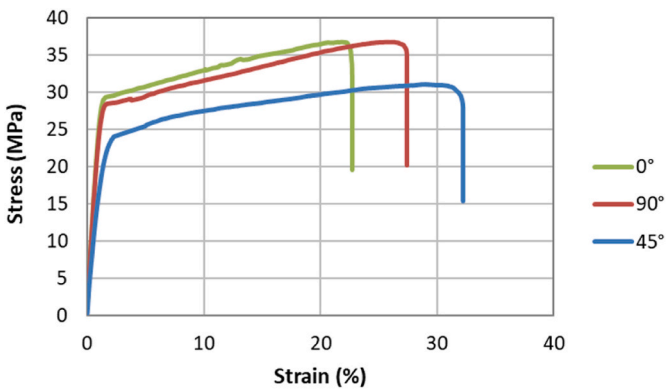

Fig. 3. Typical stress-strain plots for SRPLA loaded in 3 directions.

In the SRPLA specimens placed in seawater tanks we recorded, in the first hours of immersion, a weight gain of 2–8% percent, with considerable scatter (Fig. 4a). Our observations using SEM indicate that surface porosity may be the cause for rapid water incorporation within the SRPLA material (Fig. 5). It is postulated that these surface pores are filled within minutes. This was confirmed by additional short immersions and drying. As the amount of porosity varied between samples this resulted in large variability in weight gains. If this first weight measurement (after 9 h in water) is assumed to be solely due to instantaneous filling of free space rather than diffusion into the polymer this initial (9 h) value can be subtracted from all subsequent measurements, and with this correction more conventional plots such as those shown in Fig. 4b were obtained for the different temperatures. Saturation plateau weight gain values around 1–2% were then similar to expected weight gains based on previous PLA studies [29,30]. Corrected plots were then produced for all six immersion temperatures, based on mean weight gain measurements on five coupons at each at each time and condition (Fig. 6).

Behaviour of this SRPLA in seawater can be divided into two regimes. At temperatures above 40 °C the weight gain is rapid and causes degradation in a few days at 80 °C and a couple of weeks at 60 °C. Degradation refers here to physical separation of coupons into several pieces. The mechanisms will be described further in the Discussion section below. At temperatures below 40 °C the material saturates in a Fickian manner, and after one year at 4, 15 and 25 °C the weight gain is constant, around 1.7%. Around 40 °C there is a transition between these two regimes, with slowly increasing weight gain over 6 months followed by an acceleration and then decreasing weight gains. The form of this plot at 40 °C is similar to that shown in Ref. [29] for 40 °C seawater ageing of injected PLA specimens. It was attributed to hydrolysis, and molecular weight measurements indicated significant chain scissions. Ignoring the surface pore water and assuming Fickian diffusion at the start of immersion it is possible to determine diffusion coefficients and saturation weight gains at each temperature (Table 2).

Masses at saturation are around 1.8% for all immersion conditions. At 40 °C and 60 °C these values correspond to the level before coupon weight starts to increase. At 80 °C there is no stable weight gain value, degradation starts before saturation.

- *Changes in tensile properties with immersion time at 40 °C.*

The tensile property values measured periodically throughout the ageing period (modulus, break stress and strain), all decreased with ageing time, Fig. 7.

The modulus is less sensitive to ageing over the first 9 months than failure properties, whereas the failure stress drops progressively. The failure strain remains at a high level for about 3 months before falling to low values.

Results from two extra series should also be mentioned. First, an unaged reference series was tested at the end of the ageing period, one year after the initial tests. Results were identical to those of the unaged specimens tested initially, indicating that the material had not changed with time during room temperature storage (20 °C). Second, another set of specimens was held at 40 °C in an oven for 9 months before testing, to check that the temperature alone did not affect the tensile behaviour. The results were also identical to those of the unaged reference specimens.

- *Impact behaviour*

For many marine applications, impact is a critical loading. It is the case here for the targeted applications which are port infrastructure such as dock fenders, floating navigation buoys with a risk of collision and pleasure boat structures. Impact tests were therefore performed on dry and seawater saturated SRPLA biocomposites. The maximum energy absorbed and maximum peak force at different incident energies are

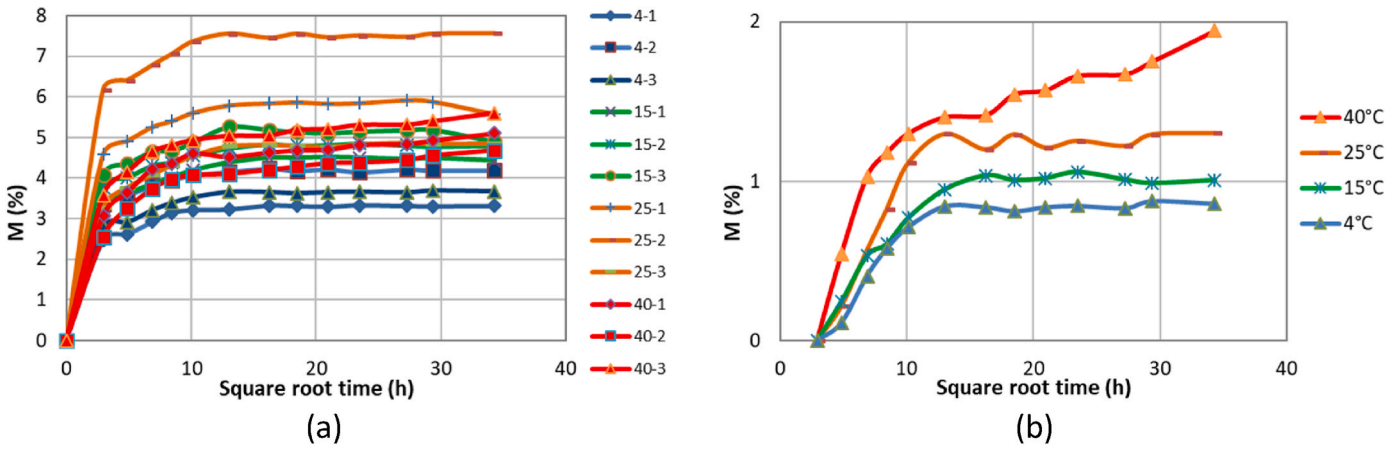

Fig. 4. Coupon weight measurements, a) raw data, b) after removal of 9 h weight values.

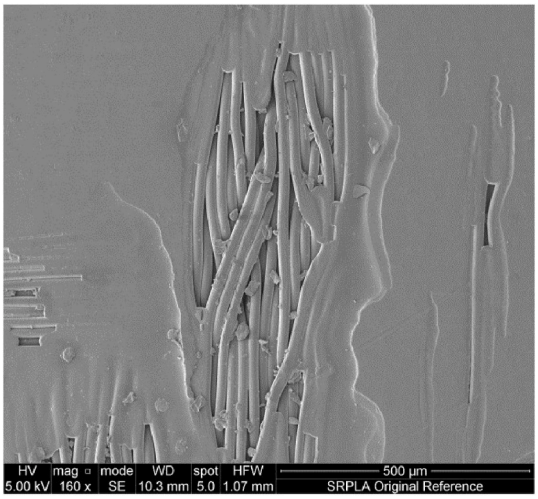

Fig. 5. SEM image showing surface porosity.

reported in Table 3.

The force-displacement, force-time and energy-time traces subjected to different impact energy levels (5, 10, and 15 J) under dry and water immersed conditions are shown in Fig. 8. As the energy levels increase, the impact force also increases for all samples. For all samples subjected to 5 J incident energy there is a barely visible impact damage indicated by force displacement curves which return to their origin or show a closed shape. This indicates that the samples absorb all the incident energy. A similar trend can be noted for dry samples and those immersed in water at 25 and 40 °C. Similar behaviour is observed for energy absorption curves at 10 J incident energy (Fig. 8 (a)), with no visible effects of moisture absorption on the impact damage. The applied energy of 5 and 10 J was not sufficient to perforate and fully penetrate the specimens. At these energy levels, all samples behaved in a similar way with similar maximum force and absorbed energy. An incident impact energy of 10 J is just enough to indent the specimens. It is worth noting that at the 5 and 10 J incident energy levels, the energy applied has been dissipated mainly through an elastic response. At 15 J, however, all the specimens, both dry and water aged, are fully penetrated, and the impact tup pierces the specimen completely.

Examples of images of front and rear faces of impacted specimens are shown in Fig. 9 (a) and 9(b) respectively. These reveal that at the 5 J and 10 J impacted points, there is only a slight whitening, which appears more pronounced after water ageing. As the energy level increases, the size of the surface indentation increases. However, for 15 J, all the samples show penetration damage. These results indicate that the

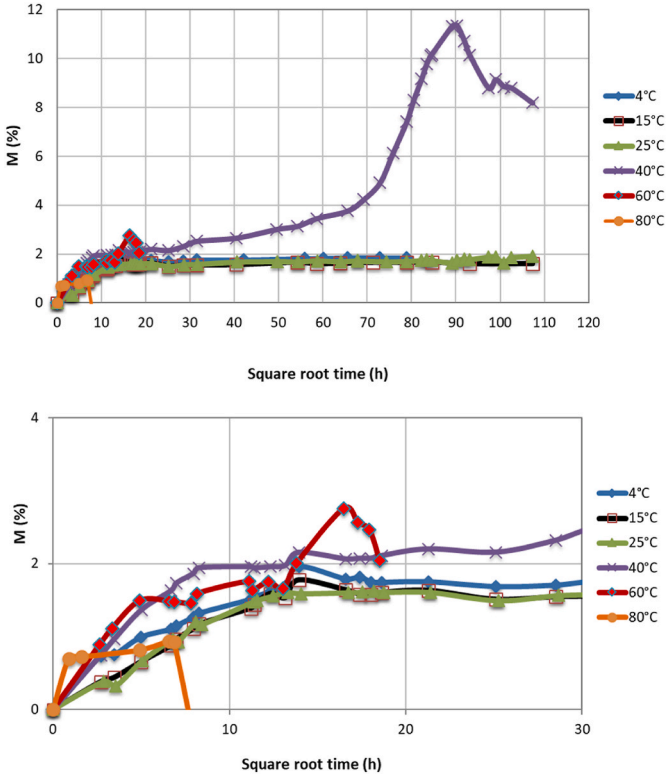

Fig. 6. SRPLA mean weight gain plots at six temperatures. Upper: complete immersion period. Lower: zoom on first month of immersion.

Table 2
Initial diffusion coefficients and saturated weight gains for different seawater immersion temperatures.

Temperature (°C)	D (m^2/s) * 10^{-12}	Ms (%)
4	0.17	1.8
15	0.53	1.7
25	0.55	1.8
40	1.56	2.1
60	3.85	1.7

impact resistance of SRPLA is not strongly affected by immersion in water. Indeed, closer examination of the fracture regions suggests that for the water immersed conditions the material fails in a more ductile fashion. The immersion durations here were quite short; for a prolonged

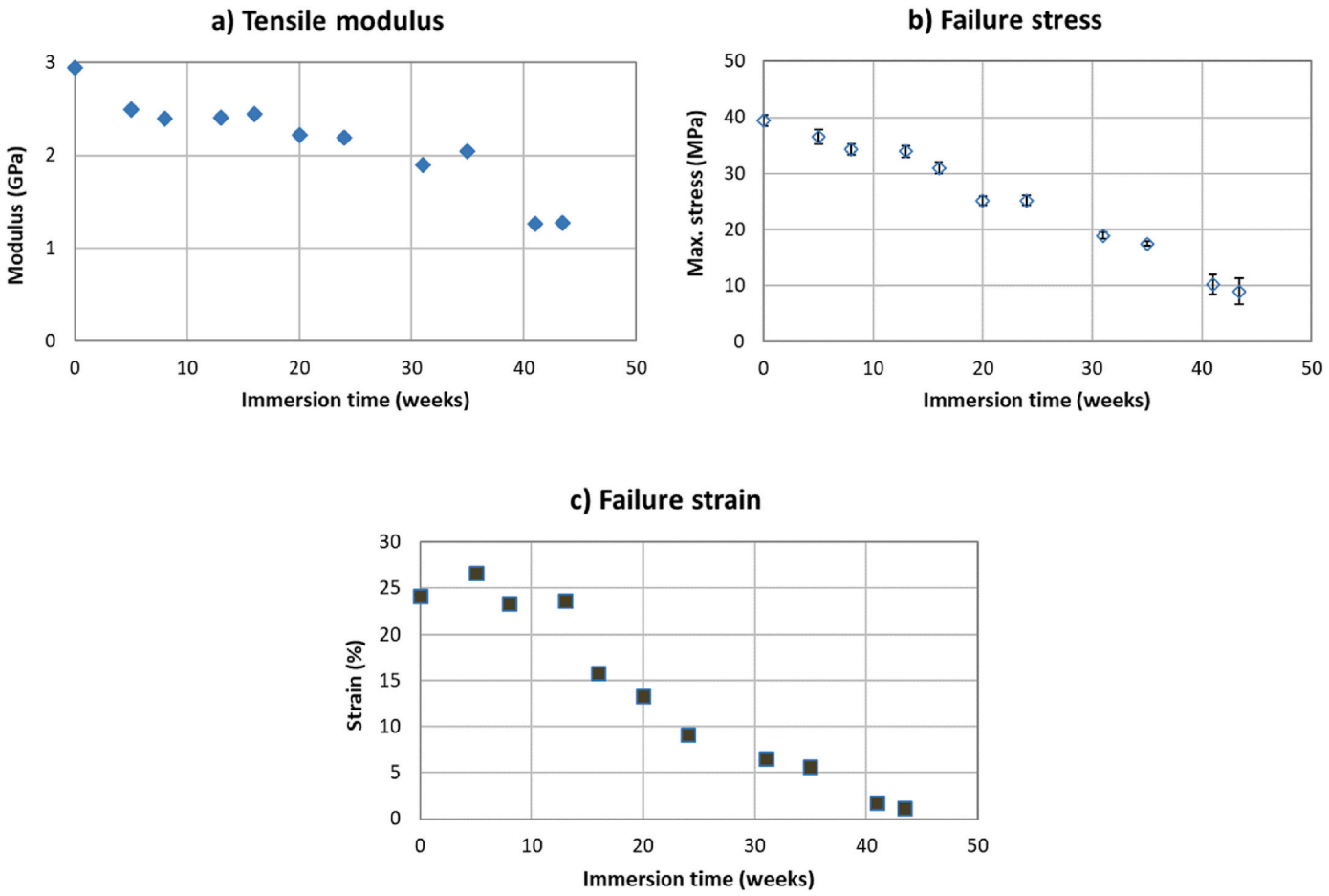

Fig. 7. Mean tensile properties during seawater immersion at 40 °C. Error bars show standard deviations.

Table 3
Summary of low-velocity falling weight impact test results for three different incident energy levels at dry, 25 and 40 °C water immersion, mean (standard deviation).

Incident energy (J)	Specimen ageing condition	Maximum absorbed energy (J)	Maximum force (N)
5	Dry	5.23 (0.03)	1172 (4)
	Water immersed 25 °C	5.24 (0.05)	1152 (3)
	Water immersed 40 °C	5.24 (0.03)	1137 (7)
10	Dry	10.73 (0.00)	1570 (18)
	Water immersed 25 °C	9.93 (0.07)	1671 (11)
	Water immersed 40 °C	9.88 (0.05)	1658 (8)
15	Dry	15.11 (0.85)	1673 (209)
	Water immersed 25 °C	10.20 (0.98)	1705 (119)
	Water immersed 40 °C	11.90 (2.65)	1838 (233)

period, the results from long seawater ageing presented above suggest that cracks would initiate, and the impact failure modes would be expected to become more brittle.

Scanning electron microscope images of samples removed from the 15 J incident energy impact samples are shown below (Fig. 10).

The local damage behaviour appears to be similar for dry and 25 °C water aged samples. For samples impacted after 40 °C ageing, there is some evidence of matrix degradation where the fibres are more exposed. Moreover, at 40 °C, PLA fibres show less distortion than at dry and 25 °C. However, there is no clear indication that at these moisture contents the ageing treatment influences the impact performance of SRPLA samples significantly.

- *Microplastic formation*

The procedure to quantify the microplastic formation described previously was judged to be suitable for its purpose as no contamination was observed, and recovery rates were high. During the entire procedure, we accounted for airborne contamination via the observation of 15 negative control samples (procedural blanks, i.e. only 20 mL Milli-Q water), in which only one SRPLA contamination particle was observed. In the recovery test, we achieved a recovery rate of 111% ± 17% (mean ± standard deviation) of SRPLA particles, which is comparable to Maes et al. [54]. After exposure to artificial seawater, SRPLA microplastics released from original flakes were observed in all samples including those subjected to Ultraviolet (UV) radiation and those sealed from UV (i.e., dark control). To confirm the polymer composition of formed microplastics, 44 particles were analysed with μ-FTIR and 33 of them were correctly visualised as SRPLA. Particles that misidentified as SRPLA were removed prior to microplastic quantification. The UV radiation had no effect on the number of formed SRPLA microplastics (Fig. 11). The average number of MP particles in "dark control" and "UV exposures" are 9 ± 5 and 17 ± 18 respectively. Within UV exposures, the average number of formed SRPLA particles was independent of UV radiation duration ($p = 0.12$; Kruskal-Wallis). The highest mean number of SRPLA microplastics was 39 ± 30 in samples after 917 h UV exposure.

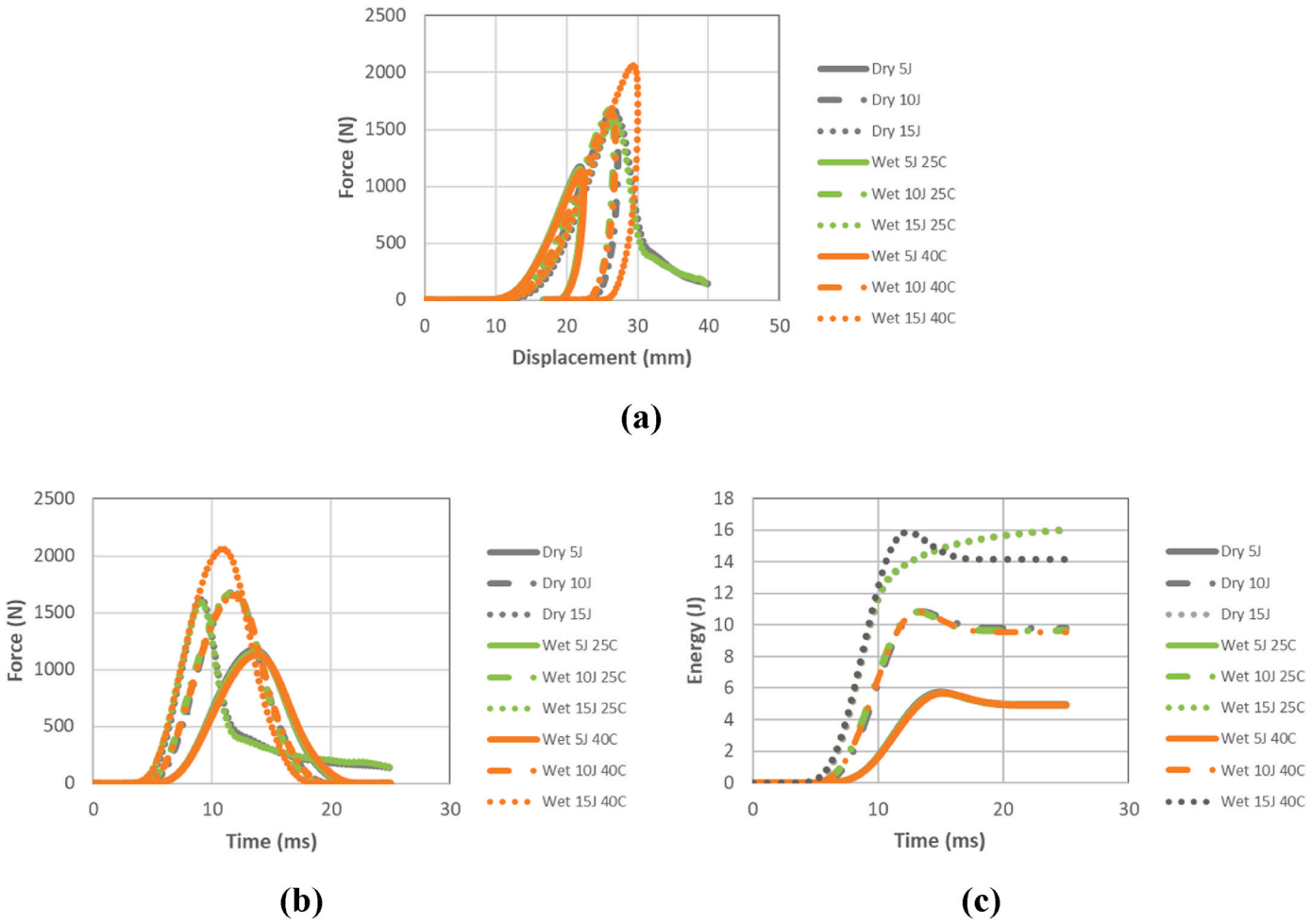

Fig. 8. Low velocity falling weight impact test results (a): force-displacement traces, (b) force-time plots and (c) energy-time plots.

4. Discussion

First, the influence of seawater on SRPLA stability will be discussed, with particular emphasis on ageing temperature. Then the suitability of this material for use in a marine environment will be considered.

4.1. Degradation of SRPLA during immersion

The results shown in this work indicate that for temperatures above the dry Tg (55–60 °C) hydrolytic degradation in water of these SRPLA is rapid, as has been shown previously in studies on composting of PLA, for example [28]. For the 60 and 80 °C immersion conditions here, extensive cracking appeared on the coupons within a few days, so that mechanical testing was no longer possible. The cracks appear to follow the fibre orientations, Fig. 12.

A first question is why does degradation occur at 40 °C ? Optical and SEM images show the damage mechanisms, Fig. 13. At a macroscopic scale large cracks are visible. Microscopic inspection reveals many surface blisters and fine cracks which appear to orignate from them. Blisters can form during wet ageing when water diffuses through an outer layer and changes in water concentration result in pressure building up within the layer by osmosis. It is a well-known phenomenon in boat-building with composites which have an outer gel-coat layer of a different chemistry to the composite matrix [55,56] but it is not clear why this should occur here.

Published results by Gil-Castell et al. [33] suggest that the glass transition temperature (Tg) drops during water immersion, in a similar way to that of polyamides, so that the material state with respect to the ageing conditions evolves with time, and after around 6 months in water the new Tg is below the 40 °C water temperature. To examine this hypothesis unaged and aged samples from the present study were analysed by DSC after drying; a small drop in Tg was measured after ageing at 40 °C, Table 4, but the values remain above the temperature of the ageing water. The reduction is much smaller than those reported in Ref. [33]; this may be due to different test conditions (sea water vs ultra-pure water) or differences in the polymer grades.

However, the darkened colour of the coupons after extended immersion at 40 °C suggests that there is an additional degradation mechanism. The samples are immerged in natural seawater, pumped from the Brest Estuary, and this contains marine microorganisms. Longer exposure to these may also contribute to degradation. In order to study this further it would be interesting to run additional tests in parallel in deionized water.

The residual properties after 40 °C immersion are plotted with respect to corrected weight gain in Fig. 14. Failure property changes are directly related to the amount of water in the material over the first 6 months, before more extensive damage develops, in the form of cracking, similar to that noted more rapidly at higher temperatures.

The sequence of damage development at different temperatures can now be described: At high temperature (60, 80 °C) hydrolysis is rapid, leads to macroscopic cracking. At 40 °C the first damage is the removal of surface matrix, with the appearance of blisters and small cracks. These expose larger surfaces to water ingress and the weight gain accelerates. The presence of mico-organisms in seawater may also contribute to degradation.

This direct correspondence between water ingress and mechanical

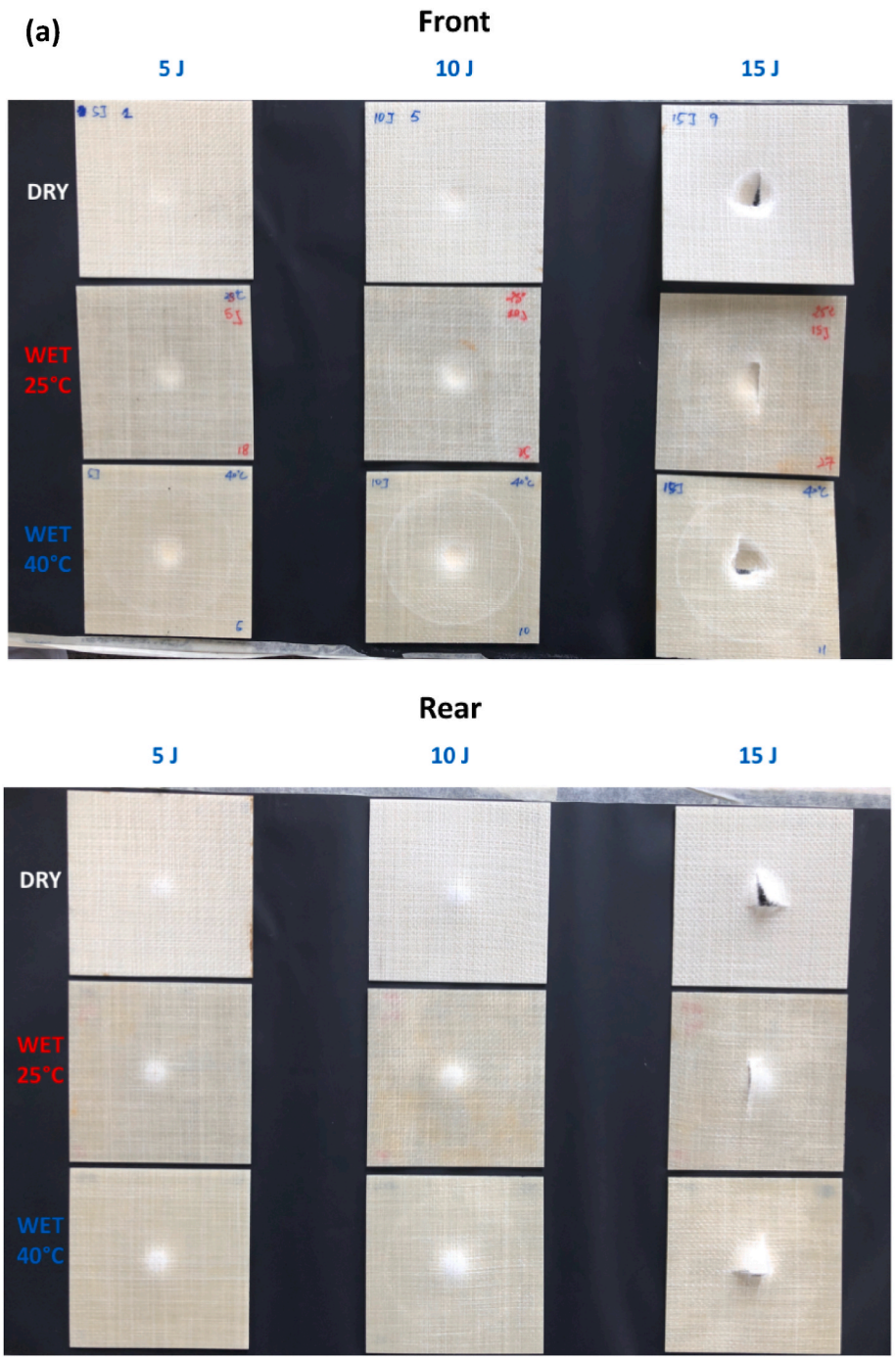

Fig. 9. Visual observations of the samples depicting their (a) front and (b) rear impacted faces respectively, with different energies (5 J, 10 J, 15 J) in dry, 25 °C and 40 °C wet aged conditions.

properties and the possibility to determine water profiles from the diffusion kinetics suggests that it will be possible to estimate lifetimes for marine structures under these conditions. However, 40 °C is a relatively high water temperature. Sea temperatures vary considerably, from around 30 °C in tropical regions to near 0 °C at the poles. Temperature also drops with depth, reaching around 5 °C in the deep oceans. The degradation rate in service will therefore depend on the location and the immersion depth. The next question which this raises is whether after sufficiently long times at lower temperatures the materials would also start to degrade ? An additional set of tests was therefore performed on wet samples which had been immersed for 12, 18, 21 and 24 months in 25 °C seawater (Fig. 15). This revealed a gradual drop in strength, with a loss after 2 years of around 23%, and degradation times around 6 times longer than at 40 °C.

The weight gain at 25 °C after 24 months in seawater has increased, from 1.7% after 1 year to more than 2% after 2 years. This figure also indicates why the transverse impact properties did not change significantly after ageing for 4 weeks in water at 25 and 40 °C: Much longer ageing times would be required to degrade these properties significantly. Within the Bio4Self project ageing tests were performed on a similar material, using an Arrhenius extrapolation from tests after ageing at different temperatures and relative humidities [57]. The results predicted that it would take about 10 years at 25 °C and 70%RH to reach a 20% reduction in tensile strength. The result in Fig. 15 shows

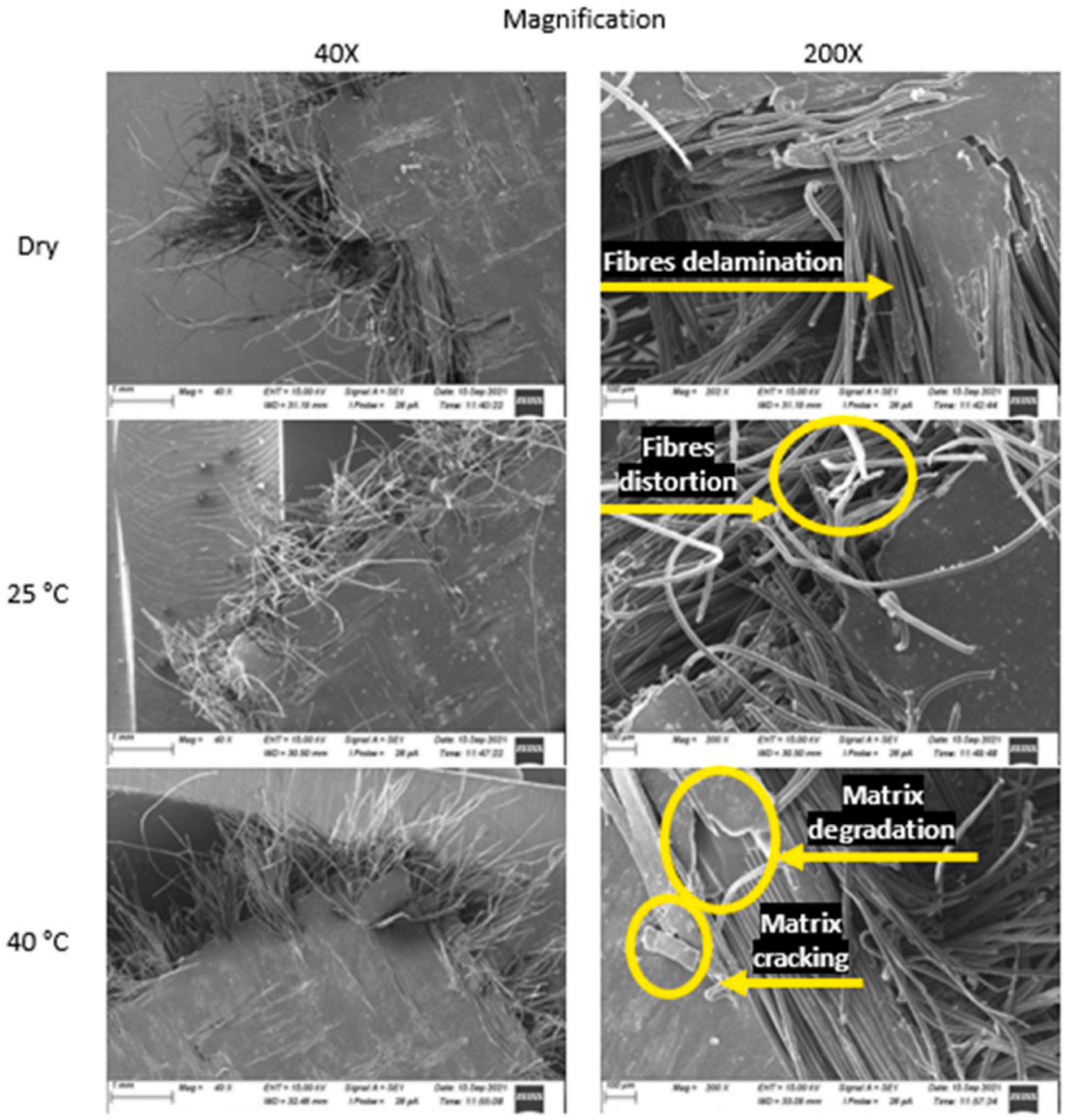

Fig. 10. SEM images of the SRPLA at dry condition and seawater ageing (25 °C and 40 °C) samples impacted at 15 J incident energy level, magnifications of 40 and 200 X

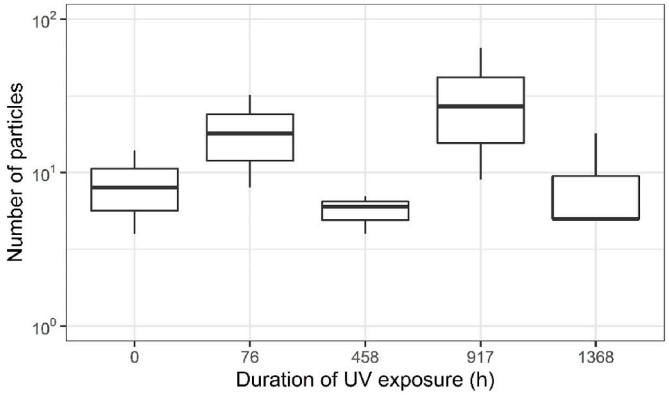

Fig. 11. Boxplot of the count of SRPLA microplastics (>50 μm) versus the duration of UV radiation (h). The number of microplastics was expressed as logarithm with a base of 10. The UV exposure "0 h" refers to "dark control".

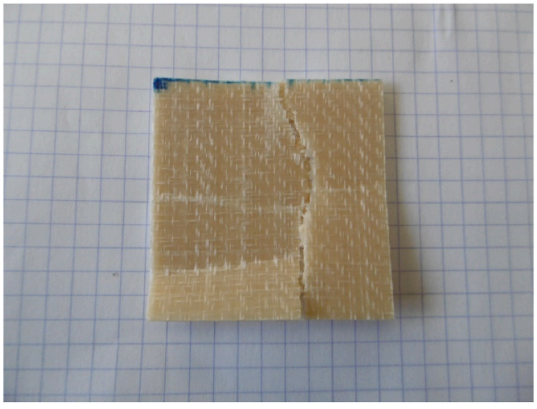

Fig. 12. Weight gain coupon immersed at 80 °C for 4 days.

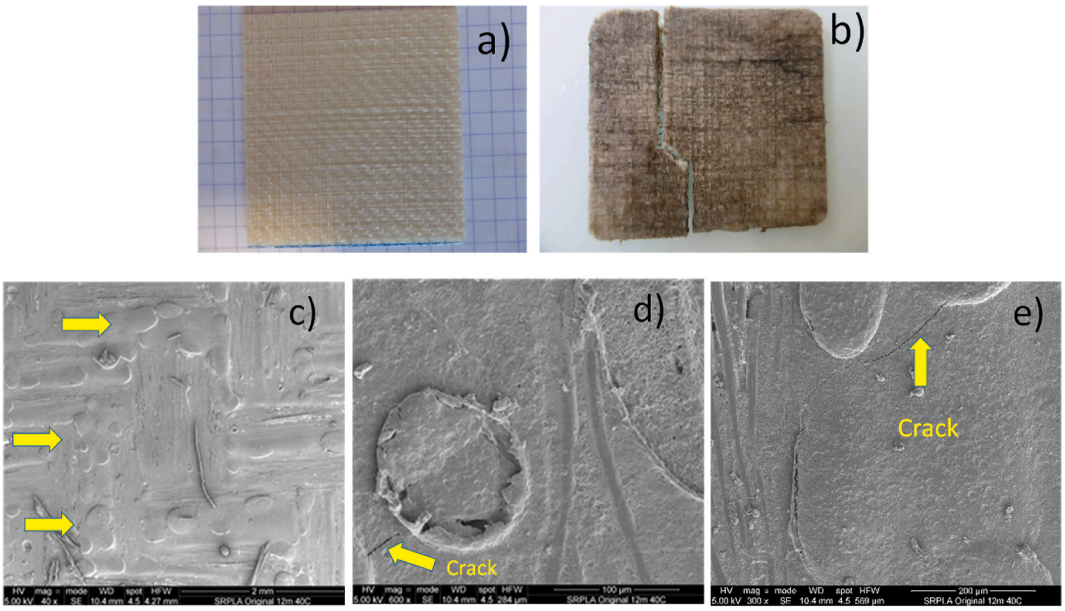

Fig. 13. Images of weight gain coupons. a) Unaged coupon. b) Coupon after 12 months 40 °C. c) Low magnification SEM coupon surface after 12 months immersion 40 °C, arrows indicate blisters. d) and e) SEM high magnification images with arrows showing cracks initiating from blisters, 12 months 40 °C.

Table 4
Values of Tg measured by calorimetry (DSC), mean (standard deviation).

Unaged Reference (°C)	24 months at 25 °C (°C)	9 months at 40 °C (°C)	12 days at 60 °C (°C)
62.4 (0.4)	61.9 (2.0)	58.1 (0.2)	55.5 (0.4)

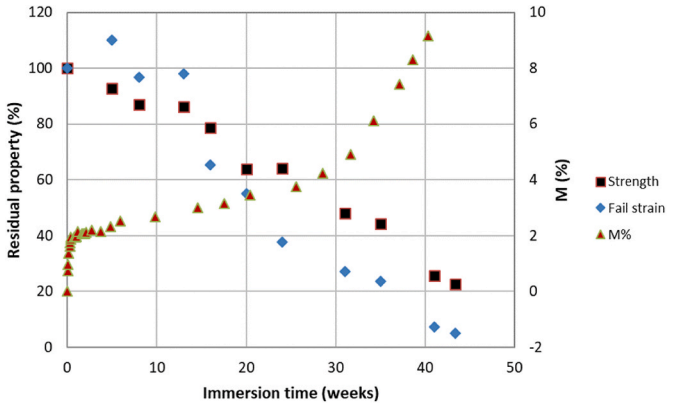

Fig. 14. Correlation between normalised loss in failure properties, after different immersion times at 40 °C, compared to initial unaged values and weight change.

that such a reduction was reached after only 2 years in natural seawater at 25 °C. This may suggest that biological factors accelerate degradation, but may also simply reflect uncertainty in extrapolating test data from a few months to longer times.

4.2. Use of the SRPLA in the marine environment

In order to evaluate new materials for marine applications it is essential to assess their degradation in the marine environment. The investigation of microplastic formation is an essential part of this evaluation. In this study, the formation of SRPLA microplastics (>50 μm) was detected in all samples after up to 1368 h exposure in artificial seawater regardless of whether subjected to UV radiation or not. The

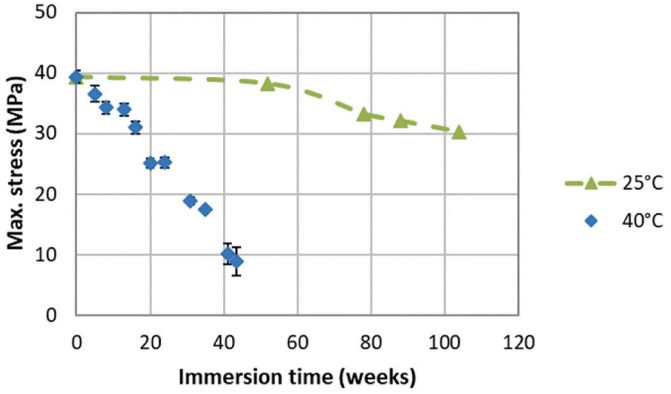

Fig. 15. Comparison between tensile response of unaged samples and samples after 12, 18, 21 and 24 months' 25 °C and 40 °C seawater immersion.

mean number of microplastic particles in "dark control" and "UV exposure" samples were 9 ± 5 (SD, n = 3) and 17 ± 18 (SD, n = 3) respectively. These results are in line with those of Lambert and Wagner [47] who exposed pieces (1 × 1 cm) of PLA disposable cups in deionized water to visible and UV light for 56 days, and found the presence of MPs (2–60 μm) both in UV treated and dark control samples. Similarly, Song et al. [48] confirmed the finding on polypropylene (PP) and expanded polystyrene (EPS) pellets after similar exposure duration. However, the number of formed microplastics in those two studies is orders of magnitude higher than in the present study. For example, the results of Lambert and Wagner [47] indicated an estimated 425 and 20,000 particles (2–60 μm)/L respectively in PLA samples in the dark and subject to 56-day UV radiation, which is up to 1000-fold of the number in the present study. The smaller number of microplastics formed from SRPLA can be expected given its durability in seawater (i.e. no significant changes in tensile properties after 8 weeks seawater immersion at 40 °C, Fig. 7). However, test specimens in literature studies are usually from commercial products (e.g. disposable PLA cups [47]) where the durability information in seawater is unavailable. It should also be noted that the targeted size range in the present study (>50 μm) is larger than the values in the work of Lambert and Wagner [47] (i.e. 0.6–18 μm and 2–60 μm) due to different microplastic identification techniques

applied. When different size ranges are compared; distinct size fractions may show a different pattern of microplastic abundance. For example, in the works of Kooi et al. [40,41], the author suggested that the abundance of microplastic in the environment follows a power law function against their particle sizes (i.e. smaller microplastics are more abundant than larger ones). Similarly, Lambert and Wagner [47] found that the concentrations of 0.6–18 μm PLA microplastics formed are up to 1000-fold of the value for 2–60 μm microplastics. Future studies are encouraged to solve such non-alignment in the quantification of microplastic formation.

Similar numbers of SRPLA microplastics were formed in samples subjected both to 1368 h UV and sealed from UV (Fig. 11), suggesting that UV radiation does not accelerate microplastic formation from SRPLA on the short term. Similarly, Lambert and Wagner [47] found PLA particle concentration (2–60 μm) did not obviously increase after 1344 h UV and daylight exposure, but a significant increase in particle concentrations were observed after 112 days. However, when compared with conventional polymers, the findings varied among polymer compositions. For example, Song et al. [48] reported that 2 months UV radiation did not affect the number of formed microplastics for PP and EPS. Exposed to the same UV dose as the present study, Sørensen et al. [44] found that polyethylene terephthalate (PET) fibres fragmented into smaller micron-sizes, indicating the formation of microplastics. So far, conclusions cannot be draw on whether SRPLA is more resistant to microplastic formation under UV radiation than conventional polymers since 1) a lack of direct comparison between SRPLA and representative conventional polymers on the number of microplastics formed under the same UV radiance dose; 2) UV radiation doses and the methods of characterising microplastic formation vary between studies. Future studies are strongly recommended to establish standardized guidelines for assessing the microplastic formation and numeric thresholds of formed microplastics, compared to reference conventional polymers, for newly developed plastic materials and applications prior to reaching the market.

5. Conclusions

This study provides new information on the stability of self-reinforced PLA in a marine environment. SRPLA is a material which is bio-sourced, and degrades rapidly at temperatures of 60 °C and higher. However, this material is quite stable in cold seawater, at temperatures of 4 and 15 °C, and retains its tensile and impact performance for short immersion durations at 25 and 40 °C. Longer immersion in seawater results in quite rapid degradation at 40 °C and slower degradation, by a factor of around 6, at 25 °C. This study has provided quantitative data for the first time to evaluate the tensile properties of SRPLA for marine applications. In parallel with the mechanical study the first results presented here for microplastic formation of SRPLA indicate that formation rates are quite low and that UV radiation does not affect their formation, but more work is needed to establish comparisons with other common plastics. Finally, the materials tested here were produced from co-mingled fibres, but there is considerable scope for innovative fabrication developments to produce SR composites from alternative feedstock such as core-sheath fibre technologies. These are currently under investigation.

Data availability

The data that has been used is in this paper is confidential at present for commercial reasons.

CRediT author statement

Maelenn LeGall: Conceptualization, Testing, Writing, Editing Zhiyue Niu: Testing, writing, editing, Marco Curto: Testing, writing, editing, Ana Isabel Catarino: Conceptualization, Writing- Reviewing and Editing, Writing-. Elke Demeyer: Writing, Reviewing, Editing. C. Jiang: Investigation, editing.: Hom Dhakal: Conceptualization, Funding acquisition, Supervision, Reviewing: Gert Everaert: Conceptualization, Funding acquisition, Supervision, Writing, Reviewing, Peter Davies: Conceptualization, Funding acquisition, Supervision, Testing, Original draft preparation- Editing.

Declaration of competing interest

The authors declare that they have no known competing financial interests or personal relationships that could have appeared to influence the work reported in this paper.

Acknowledgements

The SeaBioComp project has received funding from the Interreg 2 Seas programme 2014–2020 co-funded by the European Regional Development Fund under subsidy contract number 2506–006.

Appendix A. Supplementary data

Supplementary data to this article can be found online at https://doi.org/10.1016/j.polymertesting.2022.107619.

References

[1] C. Penu, M. Henou, Acide polylactique (PLA), Techniques de l'Ingénieur AM 3 (317) (July 2017) (in French).
[2] D. Garlotta, A literature review of poly(lactic acid), J. Polym. Environ. 9 (No. 2) (April 2001).
[3] N.J. Capiati, R. Porter, The concept of one polymer composites modelled with high density polyethylene, J. Mater. Sci. 10 (1975) 1671–1677.
[4] B. Alcock, T. Peijs, in: Technology and Development of Self-Reinforced Polymer Composites, Adv Polym Sci, Springer-Verlag Berlin Heidelberg, 2011, p. 3.
[5] C. Gao, et al., Development of self-reinforced polymer composites, Prog. Polym. Sci. 37 (6) (June 2012) 767–780.
[6] T. Stern, A. Teishev, G. Marom, Composites of polyethylene reinforced with chopped polyethylene fibres: effect of transcrystalline interphase, Compos. Sci. Technol. 57 (1997) 1009–1015.
[7] S. Pegoretti, A. Ashkar, M, C. Miglairesi, G. Marom, Relaxation processes in polyethylene fibre-reinforced polyethylene composites, Compos. Sci. Technol. 60 (2000) 1181–1189.
[8] P.J. Hine, I.M. Ward, N.D. Jordan, R. Olley, D.C. Bassett, The hot compaction behavior of woven oriented polypropylene fibres and tapes. I. Mechanical properties, Polymer 44 (2003) 1117–1131.
[9] B. Alcock, N.O. Cabrera, N.M. Barkoula, J. Loos, T. Peijs, Interfacial properties of highly oriented coextruded polypropylene tapes for the creation of recyclable all-polypropylene composites, J. Appl. Polym. Sci. 104 (2007) 118–129.
[10] N.O. Cabrera, B. Alcock, E.T.J. Klompen, T. Peijs, Filament winding of co-extruded polypropylene tapes for fully recyclable all-polypropylene composite products, Appl. Compos. Mater. 15 (2008) 27–45.
[11] N.O. Cabrera, C.T. Reynolds, B. Alcock, T. Peijs, Non-isothermal stamp forming of continuous tape reinforced all-polypropylene composite sheet, Compos A 39 (2008) 1455–1466.
[12] P. Rojanapitayakorn, P.T. Mather, A.J. Goldberg, R.A. Weiss, Optically transparent self reinforced poly(ethylene terephthalate) composites: molecular orientation and mechanical properties, Polymer 46 (2005) 761–773.
[13] J.M. Zhang, T. Peijs, Self-reinforced poly(ethylene terephthalate) composites by hot consolidation of bi-component PET yarns, Compos A 41 (2010) 964–972.
[14] J.L. Gilbert, D.S. Ney, E.P. Lautenschlager, Self reinforced composite poly (methyl methacrylate): static and fatigue properties, Biomaterials 16 (1995) 1043–1055.
[15] T. Nishina, I. Matsuda, K. Hirao, All-cellulose composite, Macromolecules 37 (2004) 7683–7687.
[16] N. Soykeabkaew, T. Nishino, T. Peijs, All-cellulose composites of regenerated cellulose fibres by surface selective dissolution, Composites Part A 40 (2009) 321–328.
[17] S.J. Eichhorn, A. Dufresne, M. Aranguren, N.E. Marcovich, J.R. Capadona, S. J. Rowan, C. Weder, W. Thielemans, M. Roman, S. Renneckar, W. Gindl, S. Veigel, J. Keckes, H. Yano, K. Abe, M. Nogi, N. Nakagaito, A. Mangalam, J. Simonsen, A. S. Benight, A. Bismarck, L.A. Berglund, T. Peijs, Review: current international research into cellulose nanofibres and nanocomposites, J. Mater. Sci. 45 (2010) 1–33.
[18] A. Majola, S. Vainionpaa, P. Rokkanen, H.-M. Mikkola, P. Tormala, Absorbable self-reinforced polylactide (SR-PLA) composite rods for fracture fixation: strength and strength retention in the bone and subcutaneous tissue of rabbits, J. Mats Sci, Materials in Medicine 3 (1992) 43–47.

[19] D. Wright-Charlesworth, D.M. Miller, I. Miskioglu, J.A. King, Nanoindentation of injection molded PLA and self-reinforced composite PLA after in vitro conditioning for three months, J. Biomed. Mater. Res. 74 (2005) 388–396.
[20] F. Mai, W. Tu, E. Bilottia, T. Peijs, Preparation and properties of self-reinforced poly(lactic acid) composites based on oriented tapes, Composites Part A 76 (Sept 2015) 145–153.
[21] T. Nishino, M. Tanaka, K. Nakamae, Elastic moduli of the crystalline regions of biodegradable polymers, Polym Prepr Jpn (Engl Ed) 49 (1) (2000). E 316-E.
[22] Kurokawa N, Atsushi H, Thermomechanical properties of highly transparent self-reinforced polylactide composites with electrospun stereocomplex polylactide nanofibers, Polymer, Vol 153, 26 Sept 2018, 214-222.
[23] S. Goutianos, L. Van der Schueren, J. Beauson, Failure mechanisms in unidirectional self-reinforced biobased composites based on high stiffness PLA fibres, Composites Part A 117 (2019) 169–179.
[24] J. Beauson, G. Schilliani, B. Madsen, L. Van der Schueren, G. Buyle, H. Knudsen, Self-reinforced poly(lactic acid) composites - processing conditions for industrial applications, in: Proceedings of 18th European Conference on Composite Materials, 2018. ECCM 2018.
[25] Thomas Köhler, T. Gries, G. Seide, Development of PLA hybrid yarns for biobased self-reinforced polymer composites, IOP Conf. Ser. Mater. Sci. Eng. 254 (2017), 042016, https://doi.org/10.1088/1757-899X/254/4/042016.
[26] Website Interreg project SeaBioComp. https://www.centexbel.be/en/projects/seabiocomp.
[27] L. Santonja-Blasco, A. Ribes-Greus, R.G. Alamo, Comparative thermal, biological and photodegradation kinetics of polylactide and effect on crystallization rates, Polym. Degrad. Stabil. 98 (3) (2013) 771–784.
[28] G. Gorrasi, R. Pantani, Effect of PLA grades and morphologies on hydrolytic degradation at composting temperature: assessment of structural modification and kinetic parameters, Polym. Degrad. Stabil. 98 (5) (2013).
[29] A. Le Duigou, P. Davies, C. Baley, Seawater ageing of flax/poly(lactic acid) biocomposites, Polym. Degrad. Stabil. 94 (7) (July 2009) 1151–1162.
[30] M. Deroiné, et al., Accelerated Ageing of Polylactide in Aqueous Environments: Comparative Study between Distilled Water and Seawater, Polymer Degradation and Stability, vol. 108, October 2014.
[31] H. Deng, C.T. Reynolds, N.O. Cabrera, N.-M. Barkoula, B. Alcock, T. Peijs, The water absorption behaviour of all-polypropylene composites and its effect on mechanical properties, Composites Part B 41 (2010) 268–275.
[32] J.D. Badia, O. Gil-Castell, A. Ribes-Greus, Long-term properties and end-of-life of polymers from renewable resources, Polym. Degrad. Stabil. 137 (2017) 25–57.
[33] O. Gil-Castell, J.D. Badia, S. Ingles-Mascaros, R. Teruel-Juanes, A. Serra, A. Ribes-Greus, Polylactide-based self-reinforced composites biodegradation: individual and combined influence of temperature, water and compost, Polym. Degrad. Stabil. 158 (2018) 40–51.
[34] B. Alcock, N.O. Cabrera, N.-M. Barkoula, Z. Wang, T. Peijs, The effect of temperature and strain rate on the impact performance of recyclable all-polypropylene composites, Composites Part B 39 (3) (2008) 537–547.
[35] J. Aurrekoetxea, M. Sarrionandia, M. Mateos, L. Aretxabaleta, Repeated low energy impact behaviour of self-reinforced polypropylene composites, Polym. Test. 30 (2) (2011) 216–221.
[36] R.A.M. Santos, L. Gorbatikh, Y. Swolfs, Commercial self-reinforced composites: a comparative study, Composites Part B 223 (15 October 2021) 109108.
[37] E. Van Sebille, F. Galgani, J.A. Van Franeker, D. Siegel, C. Wilcox, L. Lebreton, N. Maximenko, B.D. Hardesty, J.A. Van Franeker, M. Eriksen, D. Siegel, F. Galgani, K.L. Law, A global inventory of small floating plastic debris, Environ. Res. Lett. 10 (2015) 124006, https://doi.org/10.1088/1748-9326/10/12/124006.
[38] SAPEA - Science Advice for Policy by European Academies, A scientific perspective on microplastics in nature and society. Berlin. https://doi.org/10.26356/microplastics, 2019.
[39] A.A. Koelmans, P.E. Redondo-Hasselerharm, N.H.M. Nor, V.N. de Ruijter, S. M. Mintenig, M. Kooi, Risk assessment of microplastic particles, Nat. Rev. Mater. 7 (2022) 138–152, https://doi.org/10.1038/s41578-021-00411-y.
[40] M. Kooi, A.A. Koelmans, Simplifying microplastic via continuous probability distributions for size, size, shape, and density, Environ. Sci. Technol. Lett. 6 (2019) 551–557, https://doi.org/10.1021/acs.estlett.9b00379.
[41] M. Kooi, S. Primpke, S.M. Mintenig, C. Lorenz, G. Gerdts, A.A. Koelmans, Characterizing the multidimensionality of microplastics across environmental compartments, Water Res.. 202.
[42] B. Gewert, M.M. Plassmann, M. Macleod, Pathways for degradation of plastic polymers floating in the marine environment, Environ. Sci. Process. Impacts 17 (2015) 1513–1521, https://doi.org/10.1039/c5em00207a.
[43] N. Kalogerakis, K. Karkanorachaki, G. Kalogerakis, E.I. Triantafyllidi, A.D. Gotsis, P. Partsinevelos, F. Fava, Microplastics generation: onset of fragmentation of polyethylene films in marine environment mesocosms, Front. Mar. Sci. 4 (2017) 1–15.
[44] L. Sørensen, A.S. Groven, I.A. Hovsbakken, O. Del Puerto, D.F. Krause, A. Sarno, A. M. Booth, UV degradation of natural and synthetic microfibers causes fragmentation and release of polymer degradation products and chemical additives, Sci. Total Environ. 755 (2021) 143170, https://doi.org/10.1016/j.scitotenv.2020.143170.
[45] A. Jahnke, H.P.H. Arp, B.I. Escher, B. Gewert, E. Gorokhova, D. Kühnel, M. Ogonowski, A. Potthoff, C. Rummel, M. Schmitt-Jansen, E. Toorman, M. MacLeod, Reducing uncertainty and confronting ignorance about the possible impacts of weathering plastic in the marine environment, Environ. Sci. Technol. Lett. 4 (2017) 85–90.
[46] R.A. Naik, L.S. Rowles, A.I. Hossain, M. Yen, R.M. Aldossary, O.G. Apul, J. Conkle, N.B. Saleh, Microplastic particle versus fiber generation during photo-transformation in simulated seawater, Sci. Total Environ. 736 (2020) 139690.
[47] S. Lambert, M. Wagner, Formation of microscopic particles during the degradation of different polymers, Chemosphere 161 (2016) 510–517.
[48] Y.K. Song, S.H. Hong, M. Jang, G.M. Han, S.W. Jung, W.J. Shim, Combined effects of UV exposure duration and mechanical abrasion on microplastic fragmentation by polymer type, Environ. Sci. Technol. 51 (2017) 4368–4376, https://doi.org/10.1021/acs.est.6b06155.
[49] Directive (EU) 2019/904 of the European Parliament and of the Council of 5 June 2019 on the Reduction of the Impact of Certain Plastic Products on the Environment.
[50] C.-H. Shen, G.S. Springer, Moisture absorption and desorption of composite materials, in: Chapter 3 in Environmental Effects on Composite Materials, GS Springer, Technomic, 1981, pp. 15–33.
[51] Z.A. Oguz, A. Erklig, Water absorption parameters of glass/epoxy composites based on dimension effect, International Advanced Researches and Engineering Journal (2021) 202–208, 05(02).
[52] V.N. De Ruijter, P.E. Redondo-Hasselerharm, T. Gouin, A.A. Koelmans, Quality criteria for microplastic effect studies in the context of risk assessment: a critical review, Environ. Sci. Technol. 54 (2020) 11692–11705, https://doi.org/10.1021/acs.est.0c03057.
[53] S. Farah, et al., Physical and mechanical properties of PLA, and their functions in widespread applications — a comprehensive review, Adv. Drug Deliv. Rev. 107 (2016) 367–392, https://doi.org/10.1016/j.addr.2016.06.012.
[54] T. Maes, R. Jessop, N. Wellner, K. Haupt, A.G. Mayes, A rapid-screening approach to detect and quantify microplastics based on fluorescent tagging with Nile Red, Sci. Rep. 7 (2017) 1–10, https://doi.org/10.1038/srep44501.
[55] E. Walter, K.H.G. Ashbee, Osmosis in composite materials, Composites 13 (4) (Oct. 1982) 365–368.
[56] P. Castaing, L. Lemoine, Effects of water-absorption and osmotic degradation on long term behaviour of glass-fibre-reinforced polyester, Polym. Compos. 16 (5) (1995) 349–356.
[57] https://plast.dk/wp-content/uploads/2020/03/Bo-Madsen_DTU-Wind.pdf.
[58] ISO 10253, Water Quality — Marine Algal Growth Inhibition Test with Skeletonema Sp. And Phaeodactylum Tricornutum, 2016.
[59] R Core Team, R: a language and environment for statistical computing [WWW Document]. R Found. Stat. Comput. Vienna, Austria. URL, https://www.r-project.org/, 2019.